# From Muticomponent Precursor to Nanoparticle Nanoribbons of ZnO

**Zhou Gui,*,† Jian Liu,‡ Zhengzhou Wang,† Lei Song,† Yuan Hu,† Weicheng Fan,† and Daoyong Chen*,§**

*State Key Lab of Fire Science and Department of Chemistry, University of Science and Technology of China, Hefei, 230027, P. R. China, and Department of Macromolecular Science and The Key Laboratory of Molecular Engineering of Polymers, Fudan University, Shanghai 200433, P. R.China*

*Received: July 2, 2004; In Final Form: October 24, 2004*

A simple mild solution method is developed to synthesize a novel nanoribbon multicomponent precursor. A new 1-D nanostructure, porous structured nanoribbons which are self-assembled by textured ZnO nanoparticles, was found upon removal of ligand molecules from the ribbonlike precursor. The structure combines 1-dimensional geometry with nanoparticle morphology and displays porous structure because there are gaps/pores between the particles. The orientation textured structure of the ZnO nanoparticles can be formed by controlling the annealing time. The ZnO nanoparticle nanoribbons exhibit a long geometrical shape, uniformity, a high aspect ratio, and different optical activities with different nanostuctures. These findings demonstrate a convenient, simple technique for production of the novel one-dimensional semiconductor nanostructure suitable for subsequent processing into nanostructures, materials, and devices.

## Introduction

One-dimensional (1-D) nanostructure materials, such as nanotubles, nanowires, and nanoribbons, have attracted much attention due to their unique properties originating from their high surface area and low dimensionality,[1−3] as well as for applications in nanodevices.[4] Many synthetic methods have been developed to prepare various 1-D nanostructures. Zinc oxide (ZnO) is a well-known semiconductor for its wide band gap (3.37 eV) and high exciton binding energy of 60 meV at room temperature. As a consequence, it possesses unique optical, acoustical, and electronic properties which stimulate wide research interest in its potential applications.[5,6] A particularly striking recent observation is that of room-temperature lasing action in micron-sized rods,[2] highlighting the prospects of corresponding research interests in a morphologically controllable synthesis of ZnO to answer the demand for the development of novel devices.

The fact that the integrity of the building blocks (coordination complexes) is preserved during the synthesis and ultimately translated into the resulting assembled network offers numerous opportunities for designing frameworks with desirable shapes and sizes,[7] thus paving the way for establishing connections between molecular and solid morphologies. We attempt to establish a program aimed at constructing interesting morphologies by linking inorganic compounds and ligand (or organic) molecules with metal ions; the removal of ligand (or organic) guests by useful and controllable techniques is attempted to form inorganic nanomaterials with desirable shapes and sizes, which thus may shed new light on the development of suitable chemical strategies for the rational synthesis of novel 1-dimensional nanostructures with shape and size controlled. Under the proposal, we report two research results: First, a novel ribbonlike multicomponent precursor $ZnO{\cdot}0.15Zn(CH_3COO)_2{\cdot}0.85H_2O$ can be easily obtained by mixing zinc acetate and hydrazine solution at low temperature. To our knowledge, only limited kinds of multicomponent 1-D nanostructures have been synthesized until now, and the synthesis of new multicomponent 1-D nanostructures remains challenging to materials scientists.[8] Second, we present a novel 1-D nanostructure, porous structured nanoribbons which are self-assembled by high-orientation ZnO nanoparticles, upon removal of ligand molecules from the new ribbonlike precursor by annealing in air. The structure combines 1-D geometry with nanoparticle morphology and displays a porous structure because there have gaps/pores between the particles.[9] The orientation textured structure of the ZnO nanoparticles can be formed by controlling the annealing time. The ZnO nanoribbons exhibit a long geometrical shape (∼0.5 mm), uniformity, a high aspect ratio, and different optical activities with different nanostuctures.

## Experimental Section

We used a new ribbonlike precursor as the basic material to fabricate the nanoparticle nanoribons. To prepare the precursor, 50 mL of 0.1 M $Zn(CH_3COO)_2{\cdot}6H_2O$ and 50 mL of 0.15 M $NH_2{\cdot}NH_2$ was mixed and stirred for 10 min, then heated at 40 °C for 2−10 h. The aqueous solution turns slimy: large white flocculent colloid that is easily observed by naked eyes suspends in the solution. This new colloidal system is kinetically stable, and without obvious precipitation for several weeks at ambient temperature. The white precursor was collected after the mixture was centrifuged, filtrated, washed with water and alcohol, and dried at 40 °C for 24 h.

To prepare nanoparticle nanoribbons, the white precursor was heated in an oven at air atmosphere at 500 °C for 3 h. The ZnO product, porous structured nanoribbons which are self-assembled by high-orientation ZnO nanoparticles, was obtained through this thermotreatment process.

X-ray powder diffraction (XRD) analysis was conducted out on a Rigaku D/Max X-ray diffractometer with graphite mono-

* To whom correspondence should be addressed. E-mail: zgui@ustc.edu.cn and chendy@fudan.edu.cn.

† State Key Lab of Fire Science, University of Science and Technology of China.

‡ Department of Chemistry, University of Science and Technology of China.

§ Fudan University.

10.1021/jp047088d CCC: $30.25 
Published on Web 01/04/2005

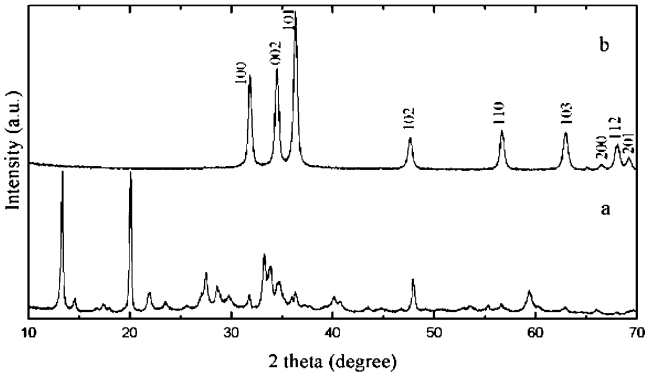


**Figure 1.** Powder X-ray diffraction pattern for (a) the precursor nanoribbons and (b) hexagonal ZnO nanoribbons.

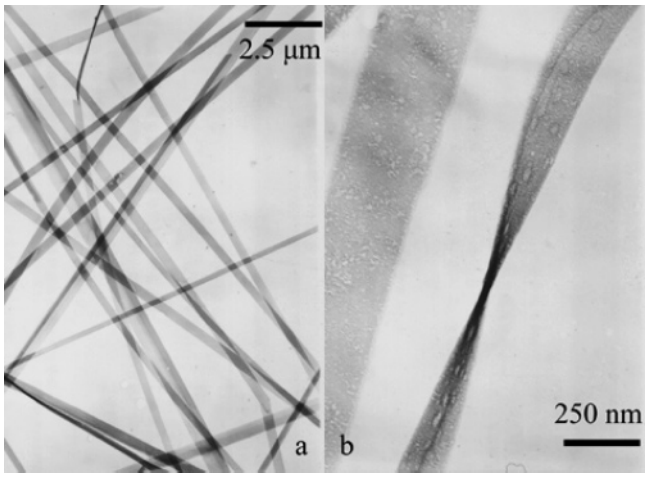


**Figure 2.** (a, b) TEM images of the precursor nanoribbons.

chromated Cu Kα radiation ($\lambda$ = 1.5418 Å). Transmission electron microscopy (TEM) images and selected area electron diffraction (SAED) patterns of the sample were collected on a Hitachi H-800 electron microscope operated at 200 keV. Scanning electron microscopy (SEM) images and X-ray energy dispersion spectrum (EDS) analysis were recorded on a JSM-6700F scanning electron microscope, working at 100 keV acceleration voltages. C, H, and N analysis was carried out by means of combustion test methods on an Elementar Vario EL-III. Zn analysis was carried out with an ICP-atomic emission spectrometer. FTIR spectra were recorded on a MAGNA-IR750 FTIR spectrometer in a KBr matrix in the range from 400 to 4000 $cm^{-1}$. Thermogravimetric (TG) analyses of the precursor samples were carried out with a Netzsch STA 409C in a flowing air atmosphere at a temperature range from 25 to 500 °C. The surface area and porosity of the samples were collected on a Coulter Omnisorp 100CX specific surface analyzer. The room-temperature photoluminescence (PL) spectra were performed on a JY-Labram spectrometer with a He−Cd laser focused at about 1 $\mu$m as the exciting source at 325 nm.

## Results and Discussion

X-ray diffraction (XRD) patterns of different products are shown in Figure 1. Figure 1a shows that a new molecular precursor was obtained at 40 °C. Transmission electron microscopy (TEM) observation in Figure 2a,b reveals that the precursors only consist of a large quantity of ribbonlike nanostuctures with typical lengths on the order of millimeters. No other morphologies such as particles, wires, et al. were detected in the samples. Each nanoribbon has a uniform width along its entire length; the typical widths and thicknesses of the nanoribbons are in the range of 300 to 500 nm and 15 to 20 nm, respectively. From Figure 2b, the many spots on the ribbons indicate that the precursors are unstable under irradiation by a strong electron beam.

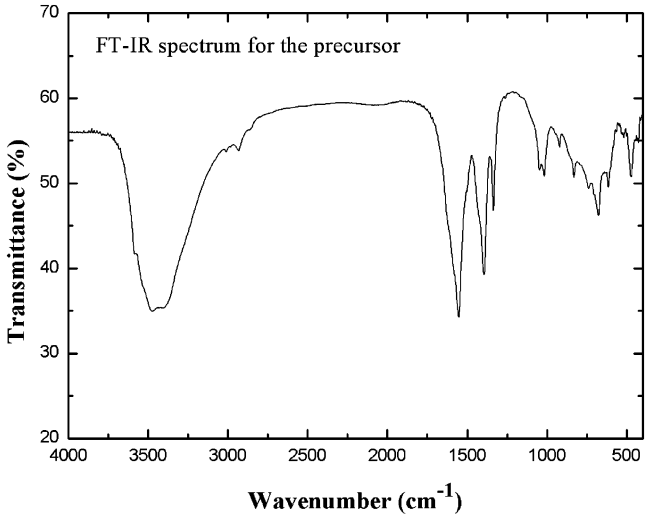


**Figure 3.** FT-infrared spectrum of the precursor sample.

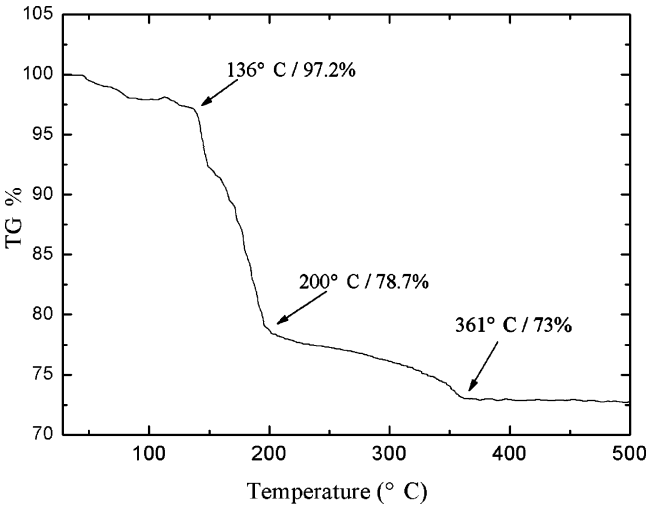


**Figure 4.** TG curve for the precursor sample between 25 and 500 °C.

The FT-infrared (FTIR) spectrum for the precursor sample as shown in Figure 3 indicates the existence of O−H vibrations and various acetate vibrations and rocks. The elemental analysis shows that the composition of the precursor can be expressed by the formula $ZnO{\cdot}0.15Zn(CH_3COO)_2{\cdot}0.85H_2O$, but the structure of the new nanoribbonlike precursor still needs to be studied in future work. Thermogravimetry (TG) analysis (Figure 4) conducted in a flowing air atmosphere shows a weight loss of ∼27% up to 361 °C, which is related to the procedure of dehydration and acetate molecule removal. The white residues of TG for the precursors were confirmed to be the pure wurtzite ZnO phase by XRD analysis.

Although the hydrazine molecules cannot be found in the precursor samples, which is different from the previous report,[10] the strong ligand hydrazine plays an important role in the formation of the 1-D nanoribbon structure. At the nucleation stage, there has been strong interaction of the electron-donating bidentate ligands with specific crystal facets.[11,12] So at the crystal growth stage, the growth on these specific facets is restricted due to preferential ligand binding. The accumulation of the atoms is faster on the unique facets, especially along the ribbon

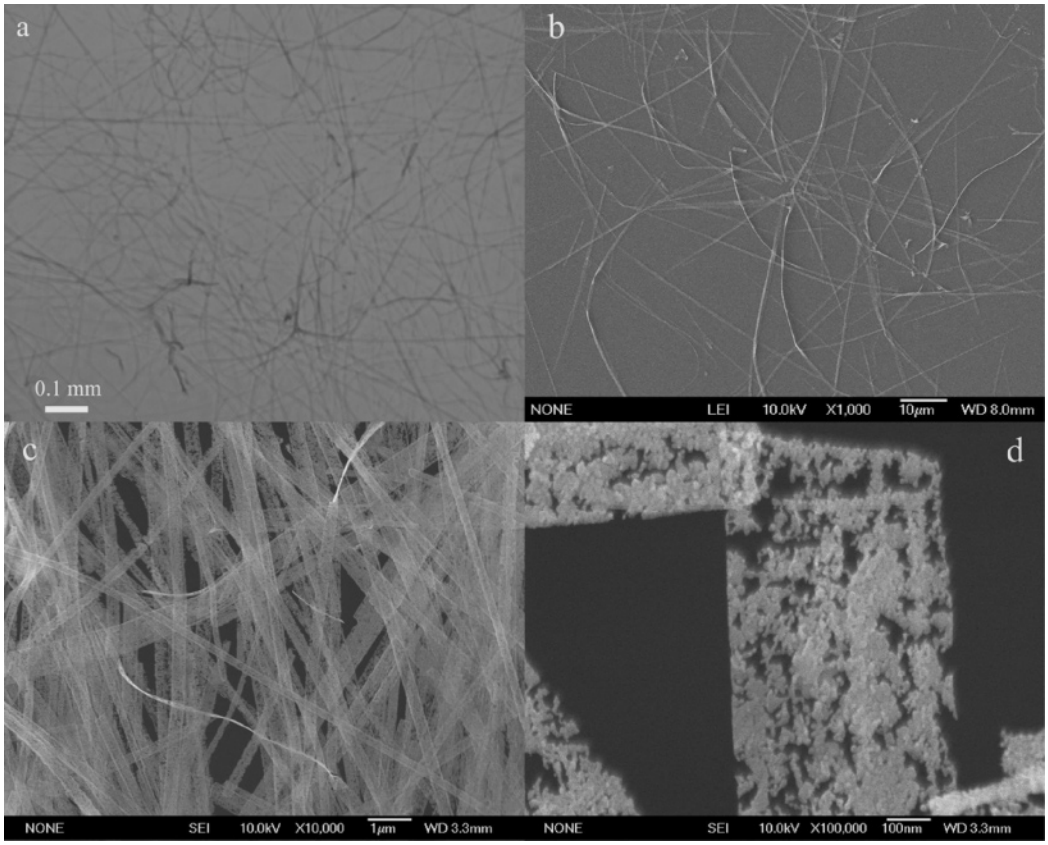


**Figure 5.** (a) Optical micrograph at 400 × showing long geometrical shape and (b−d) SEM images at different magnification revealing the ribbonlike morphology of ZnO product, which is self-assembled by nanoparticles.

axis.[11] In the end, the 1-D nanoribbon structure is formed. It should be pointed out that the length of the hydrocarbon chain of the bidentate ligands and the reaction temperature are also two key factors that determine the feasibility of the reaction of the precursor product. We respectively replaced the hydrazine by ethylenediamine or 1,6-hexamethylendiamine with a longer hydrocarbon chain, keeping other experimental variables unchanged. In the ethylenediamine and zinc acetate solution system, the product is the same as that of the hydrazine system. But in 1,6-hexamethylendiamine system, the product is ZnO nanoparticles, which was confirmed by XRD and ED analysis. When the reaction temperature for the hydrazine and zinc acetate solution system was elevated to as high as 70 °C, only ZnO was produced.

To prepare nanoparticle nanoribbons of ZnO, the white precursor was heated in an oven at air atmosphere at 500 °C for 3 h according to the data of TG. Figure 1b shows a typical XRD pattern of the ZnO nanoribbons. All diffraction peaks can be indexed to a hexagonal structure of the bulk ZnO. No characteristic peaks from other crystalline forms are detected in the XRD pattern. The morphology of the products was examined with an optical microscope (OM) and a scanning electron microscope (SEM). From Figure 5a, it is easy to observe the samples in high yield with retention of the long geometrical shape (∼0.5 mm) under ordinary OM (at 400× ). Figure 5b−d shows SEM images of ZnO nanoribbons which adopt the ribbon morphology as their precursor and nonoparticles can be detected on the ribbons. The TEM images (Figure 6a−d) confirm that the ribbon structure is composed of a large number of individual nanocrystals. These ZnO nanoparticles are self-assembled to form a closely packed nanocrystal layer. The average size of the nanocrystalline particles is 15−20 nm. There are gaps/pores between the nanocrystallites which indicate that nanoribbons display a porous structure.[9] When the electron beam was perpendicular to a ZnO ribbon surface and the electron irradiation area was adjusted to cover dozens of nanoparticles, the transmission electron diffraction (ED) pattern (Figure 6e) showed clear spots, which implies all the nanopaticles on the nanoribbon adopted the same crystallographic direction [001]. The top and bottom surface of the ZnO nanoribbon is enclosed by the (001) plane. EDS analysis of this product shows the presence of Zn and O, but the content of O is high, possibly originating from the unavoidable surface adsorption due to the porous structure of the ribbons. In research where the surface area and pore size distribution of this porous structure, which is critical for potential physical applications, for example, gas sensors,[13] BET analysis was carried out. From the sorption data, the BET surface area is calculated to be about 13.3 $m^2\ g^{-1}$. Barrett−Joyner−Halenda calculations for the pore size distribution, derived from desorption data, reveal a distribution for the sample around 25 nm.

The products, with unique 1-D porous nanoribbon nanostructure self-assembled by textured ZnO nanocrystalline, have average widths of 300−500 nm and thicknesses of 15−20 nm (the particle size) with large length-to-width ratios (∼1 000) and gigantic length-to-thickness ratios (∼25 000). With an elevated temperature, the precursor is converted directly into the thermodynamically most stable hexagonal ZnO. In this process, the precursor nanoribbons undergo dehydration and loss of small organic molecules, there is a significant shrinkage in the ribbons, then lots of many nanocrystals and gaps/pores between them form simultaneously. The removal of binding water and small organic molecules does not damage the regular arrangement of Zn, O atoms, and heating may provide the energy to make the ZnO nanoparticles self-assembled with high orientation. The reason the product of ZnO still follows the

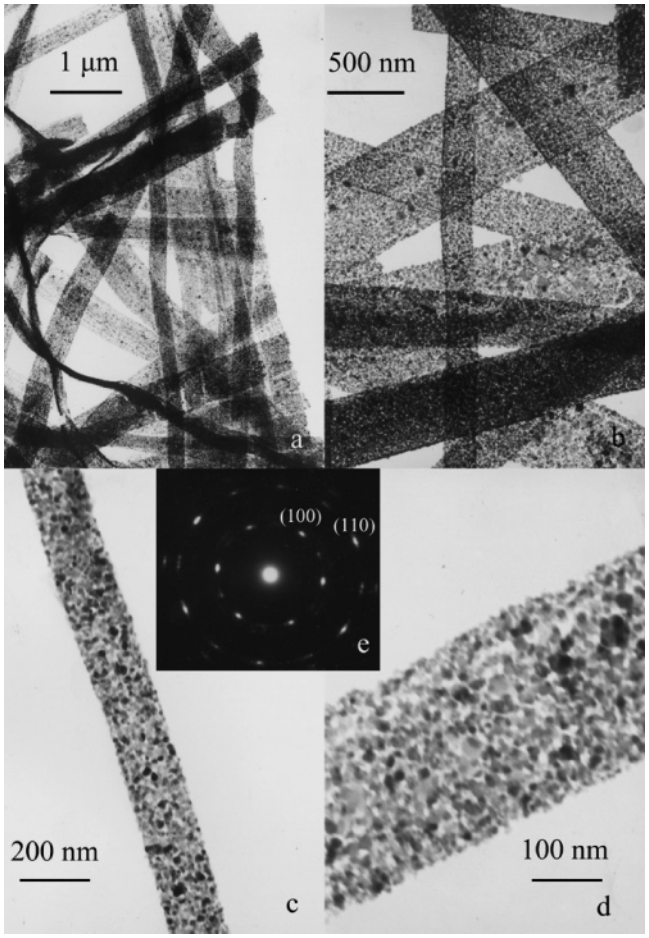


**Figure 6.** (a−d) TEM images at different magnification showing ZnO nanoribbon self-assembled by nanoparticles and (e) ED pattern of dozens of ZnO nanopaticles revealing high orientation of the nanoparticles on a ribbon.

ribbonlike morphology and keeps the long geometrical shape (∼0.5 mm) is due to there being nanocontact between each nanoparticle (Figures 5d and 6d) to stabilize the structure mechanically against collapse or fracture during the removal of the binding of water and small organic molecules .[14]

Our experimental data prove that the long annealing time (3 h) is in favor of the formation of textured structure (Figure 6e), which may lead to a gain in lattice-free energy and in the stability of nanoribbons. The short annealing time (1 h) of the precursor is conducive to no orientation of the nanoparticles on the ribbons (Figure 7 inset), which is analogous to that of nanoparticl assembly[15,16] and no other changes of the ZnO product, such as component, morphology, size of the nanoparticles, et al. So in this case, controlling the annealing time can control the high-orientation arrangement of nanoparticles.

It is easy to take PL spectra of a single nanoribbon by adjusting the laser beam on the single ribbon under the optical microscope due to the long geometrical shape and 300−500 nm width of the ZnO nanoribbons we synthesized (Figure 5a). Two samples were collected from precursor ribbons prepared on a glass slide, then annealed at 500 °C in air atmosphere for 1 h, in which there is no orientation textured nanostructure (Figure 7 inset), and for 3 h, in which nanoparticles on the ribbons exhibit textured orientation (Figure 6e). As is shown in Figure 7, PL measurements were recorded with different annealing treatments to investigate the influence of nanostructure on the emission. Strong UV band-edge emission was observed

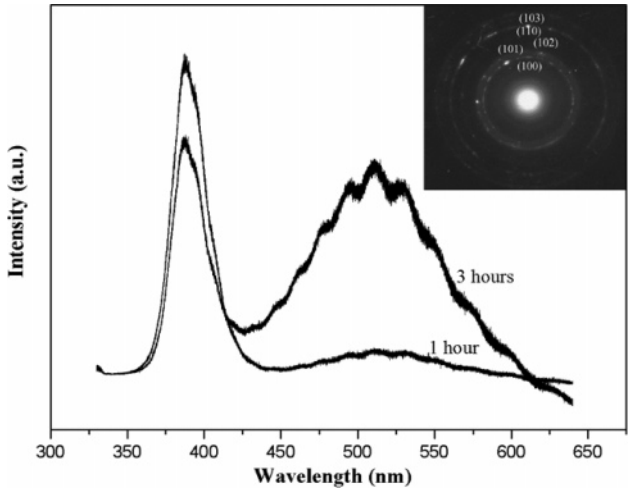


**Figure 7.** Room-temperature photoluminescence spectra of a single ZnO nanoribbon in different structures at controlled annealing times of 1 and 3 h. The inset is an ED pattern of dozens of ZnO nanopaticles on a nanoribbon with anneal time for 1 h revealing no orientation textured nanostructure on a ribbon.

at ∼385 nm resulting from free-exciton annihilation for all two samples. However, we observed that the green light emission intensity at ∼515 nm increased remarkably as the orientation textured nanostructure formed. When the pumping laser power was decreased, the PL emissions show the same results. The green emission originates from the radiative recombination of a photogenerated hole with an electron occupying the oxygen vacancy.[2,17] The remarkable increase of the green emission as the textured structure formed suggests that there is a large fraction of oxygen vacancies in the orientation textured structure of the ZnO nanocrystals with long time annealing in air. The dependence of the PL intensity[18] on incidence angle (0−90°) that the pump beam is focused on the nanoribbon to the oriented direction of ZnO nanoparticles should be an interesting subject in our future work.

## Conclusion

In summary, we have demonstrated that a novel nanoribbon multicomponent precursor can be rapidly produced with high yield under mild conditions and a novel nanostructure is presented, which combines 1-D geometry with nanoparticle morphology and displays a porous structure. These findings demonstrate a convenient, simple technique for production of a novel 1-D semiconductor nanostructure suitable for subsequent processing into nanostructures, materials, and devices. The simple chemical synthetic method, low cost, large quantity and uniformity of products, long geometrical shape, and high aspect ratio also make it possible to use the ZnO nanoribbons as nanodevices in nanoscale optoelectronic applications.

**Acknowledgment.** This work was supported by the China NKBRSF project (No. 2001CB409600) and the special foundation of State Key Lab of Fire Science.

## References and Notes

(1) Ruecks, T.; Kim, K.; Joselevich, E.; Tseng, G. Y.; Cheung, C.; Lieber, C. M. *Science* **2000**, *289*, 94.

(2) Huang, M. H.; Mao, S.; Feick, H.; Yan, H.; Wu, Y.; Kind, H.; Weber, E.; Russo, R.; Yang, P. *Science* **2001**, *292*, 1897.

(3) Pan, Z. W.; Dai, Z. R.; Wang, Z. L. *Science* **2001**, *291*, 1947.

(4) Xia, Y.; Yang, P.; Sun, Y.; Wu, Y.; Mayers, B.; Gates, B.; Yin, Y.; Kim, F.; Yan, H. *Adv. Mater.* **2003**, *15*, 353.

(5) Hiramatsu, M.; Imaeda, K.; Horio, N.; Nawata, M. *J. Vac. Sci. Technol.* **1998**, *A16*, 669.
(6) Kadota, M. *Jpn. J. Appl. Phys. Part 1* **1997**, *36*, 3076.
(7) Yaghi, O. M.; Li, H.; Davis, C.; Richardson, D. T.; Groy, L. *Acc. Chem. Res.* **1998**, *31*, 474.
(8) Yu, J.; Yu, J. C.; Ho, W.; Wu, L.; Wang, X. *J. Am. Chem. Soc.* **2004**, *126*, 3422.
(9) Gao, P.; Wang, Z. L. *J. Am. Chem. Soc.* **2003**, *125*, 11299.
(10) Yu, S. H.; Yoshimura, M. *Adv. Mater.* **2002**, *14*, 296.
(11) Peng, Z. A.; Peng, X. G. *J. Am. Chem. Soc.* **2001**, *123*, 1389.
(12) Li, Y. D.; Sui, M.; Ding, Y.; Zhang, G. H.; Zhuang, J.; Wang, C. *Adv. Mater.* **2000**, *12*, 818.
(13) Wan, Q.; Li, Q. H.; Chen, Y. J.; Wang, T. H.; He, X. L.; Li, J. P.; Lin, C. L. *Appl. Phys. Lett.* **2004**, *84*, 3654.
(14) Gui, Z.; Fan, R.; Mo, W.; Chen, X.; Yang, L.; Zhang, S.; Hu, Y.; Wang, Z.; Fan, W. *Chem. Mater.* **2002**, *14*, 5053.
(15) Lahav, M.; Sehayek, T.; Vaskevich, A.; Rubinstein, I. *Angew. Chem., Int. Ed.* **2003**, *42*, 5575.
(16) Leontidis, E.; Orphanou, M.; Leodidou, T.; Krumeich, F.; Caseri,W. *Nano Lett.* **2003**, *3*, 569.
(17) Huang, M. H.; Wu, Y. Y.; Feick, H. N.; Tran, N.; Weber, E.; Yang, P. D. *Adv. Mater.* **2001**, *13*, 113.
(18) Wang, X.; Summers, C. J.; Wang, Z. L. *Nano Lett.* **2004**, *4*, 423.